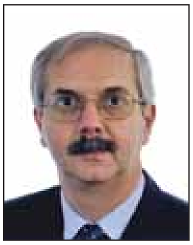

# Practical Papers, Articles and Application Notes

*Flavio Canavero, Technical Editor*

Although readers are already familiar with this Section, I would like to repeat its objective, which is to disseminate practical information to the EMC community. The material published in this Section need not be entirely original or archival, it is only necessary that the material be useful for the EMC community, either by informing the members of new applications and/or methodologies, or by educating the readers with explanations of phenomena or interpretation of experimental evidence.

While I will personally solicit contributions, I encourage all readers to actively contribute to this column, either submitting manuscripts they deem appropriate, or encouraging other authors to share something exciting with the community. I will follow up on all suggestions, and with the help of independent reviewers, I sincerely hope to publish enjoyable and instructive papers. Please communicate with me, preferably by email, at canavero@ieee.org.

The paper in this current issue is related to technological solutions for EMC. This paper represents the legacy of my predecessor, Professor Robert Olsen, to whom I am indebted for having invited the authors to contribute to the Newsletter and for having conducted the review process.

The paper is entitled "Feasibility of New Nanolayered Transparent Thin Films for Active Shielding of Low Frequency Magnetic Field" by M. D'Amore, M.S. Sarto, A. Tamburrano, and F. Sarto. The distinctive elements of this contribution are twofold: transparency of shielding material, and a realization by means of a nanoscale technology. The attractiveness of the first feature (transparency) is self-evident, since it helps solve those problems for which both shielding and the need for visual inspection and information display are unavoidable. On the other hand, nanotechnology – although in its infancy – has a great potential, and can provide engineers in the future with wonderful materials.

# Feasibility of New Nanolayered Transparent Thin Films for Active Shielding of Low Frequency Magnetic Field

*M. D'Amore, M.S. Sarto, A. Tamburrano*
*Dept. of Electrical Engineering*
*Univ. of Rome "La Sapienza"*
*Rome, Italy*
*alessio.tamburrano@uniroma1.it*

*F. Sarto*
*Advanced Physical Technologies Unit*
*ENEA R.C. Casaccia*
*Rome, Italy*

*Abstract—The feasibility of low-frequency magnetic field active shielding by using transparent metals is investigated. The basics of transparent metals and of the nanotechnology exploited to realize a test sample made of silver and titanium oxide are provided. The design of the shield is carried out by evaluating the maximum current capability of the transparent metal as function of the working temperature in order to assess the performance of the proposed new active shielding technique, which avoids the use of bulk conductors for the current flow. The sensitivity analysis of the efficiency of the transparent active shield proposed is performed by numerical simulations, considering a 2D-test enclosure with an optical aperture, excited by an inner a.c. current source at 50 Hz.*

*Keywords - Nanotechnology; thin film; low-frequency magnetic field; shielding; transparent shields.*

## I. INTRODUCTION

The low-frequency magnetic field produced by power apparatus or cable lines can originate electromagnetic interferences to nearby equipment as well as electromagnetic pollution levels that can be critical for human exposure. Numerous studies have been carried out in order to develop efficient shielding techniques for low frequency magnetic field. Both passive and active, or hybrid-screening solutions have been proposed [1] - [4].

One critical aspect concerns the magnetic field shielding when the optical access to the emitting source is required. Examples are videos and display of switching panels [4] and power filters, windows of train craft [5] or buildings. In these cases passive screening is difficult due to the fact that thick layer of metal does not allow propagation of light. Traditional active shielding solutions can be efficient from the electromagnetic (EM) point of view, but in general they always require the installation of conducting wires that constitute an optical barrier.

An innovative shielding technique against EM fields at radio frequency, transparent in the visible range, was proposed in [6], [7]. It was demonstrated that transparent metals, constituted by alternating layers of dielectric and metal, provide EM shielding of 40 dB in the frequency range from about 10 MHz to 6 GHz, and maximum optical transmittance in the visible range of 70 %.

The scope of this paper is to demonstrate the feasibility and efficiency of an innovative shielding technique for low-frequency magnetic field, based on the use of transparent metals. The proposed active screening solution, which guarantees high optical transmittance in the visible range, is particularly suitable for the shielding of windows, displays and glass walls. It avoids the installation of wire grids, which are necessary in traditional active shielding solutions.

The transparent metal coating is applied over the surface to be screened and it constitutes the conducting path for the current of the active shield circuit. In order to achieve uniformity of the chromatic resolution and optical transmittance of the screened surface, dielectric filter coatings having the same optical transparency can be applied in the areas not covered by the transparent metal.

In the following at first the basics of transparent metals and of the nanotechnology exploited to produce test samples is provided. Then, the performances of the realized specimen used for the active shielding are described in terms of the current carrying capability and optical transmittance in the visible range. Finally, the sensitivity study of the screening efficiency of active shielding solutions applied to a 2D-test enclosure with an optical aperture, excited by an inner a.c. current source at 50 Hz is performed.

## II. NANOLAYERED TRANSPARENT THIN FILMS

### A. Nanotechnology of Transparent Thin Films

Transparent metals are constituted by a periodic sequence of metallic and dielectric or semi-conducting layers [6] – [8]. They are one-dimensional (1D) photonic band gap (PBG) structures.

The materials used to realize such multilayered structures can be silver (Ag) as metal, zinc oxide (ZnO) as semiconductor, and titanium oxide ($TiO_2$) as dielectric. Ag is chosen because the location of its plasma resonance, at about 320 nm, makes it more suitable for transmission windows in the visible range than other metals [9]. ZnO is chosen as interlayer material because it is characterized by a relatively low extinction coefficient compared to other semiconductor materials, such as indium tin oxide (ITO) [10]. $TiO_2$ is generally preferred with respect to other dielectrics due to the high refraction index in the visible range.

The essential property of PBGs is that some wavelength ranges are missing in transmission, being completely reflected. In [8] it was demonstrated that a resonance tunneling mechanism allows optical waves to propagate through a 1D-PBG in which the total metal content is several skin depths or hundreds of nanometers, in thickness. This mechanism enhances the transmission by several magnitude orders, thus allowing the use of metals in optical devices.

The nanotechnology exploited to realize the transparent metals is the dual ion beam sputtering (DIBS), which is available in the Thin Film Laboratory of ENEA Research Center. The deposition process is described in detail in [6] and [7].

The optical and shielding performances of transparent metals have been widely investigated within a two-year research project. Electromagnetic coatings providing shielding effectiveness of 40 dB at radio frequency up to a few GHz and maximum optical transmittance higher than 70% for normal incidence have been realized and tested [6], [7], [11]. The critical aspect of bonding has been investigated in order to achieve the best shielding performance [12].

In this paper the asymmetrical transparent metal configuration described in [12] is considered as starting design of the active shield configuration.

### B. Sample Realization

The transparent metal sample is realized in the Thin Film Laboratory of ENEA Research Center Casaccia. The nanolayered film is deposited on a glass substrate having dimensions of 35 mm $\times$10 mm.

At first, rectangular nickel contacts, 10 mm $\times$ 5 mm in size, are deposited by DIBS at both edges of the rectangular sample; the thickness of the Ni-coating is 0.5 μm.

Next, the $TiO_2$ – Ag transparent metal is sputtered on the substrate over an area of ($l$=30 mm)$\times$($w$=3 mm), which partially overlaps the Ni-contacts. The realized specimen is sketched in Fig.1(a). Notice that the first deposited layer is a silver film. Between adjacent layers of $TiO_2$ and Ag, a thin film of Ti, having the thickness of 1 nm, is deposited in order to prevent oxidation of silver due to the migration of oxygen from the titanium oxide. The deposition error on the film thickness is ± 2 nm for $TiO_2$, ± 1 nm for Ag, and ± 0.5 nm for Ti. The different error ranges are due to the different deposition times and growth rates of the different target materials used.

The realized nanolayered coating constitutes the current path in the active shield configuration instead of traditional bulk conductors. The current is injected in the Ag layer deposited on the substrate through the Ni-contact, and flows out along the $y$-axis. The d.c. resistance offered by the $j$-th Ag layer is:

$$R_{Ag,j} = \frac{l}{\sigma_{Ag} w d_{Ag,j}} \quad j = 1.4 \qquad (1)$$

where $\sigma_{Ag}$ is the electrical conductivity of the Ag film, $d_{Ag,j}$ the thickness of the $j$-th layer, $l$=30 mm and $w$=3 mm are the length and width of the current path. The value of $\sigma_{Ag}$ = 7.75 $\cdot 10^6$ S/m is measured at the environment temperature by applying the four-point test method on an Ag film sample having thickness of 17 nm.

The equivalent d.c. resistance $R_{eq}$ measured for the realized sample is about 20 Ω. The obtained value demonstrates that $R_{eq}$ is little bit higher than the theoretical value (18.9 Ω) of the d.c. resistance of a single layer film of Ag having the electrical conductivity $\sigma_{Ag}$, cross-section to current flow ($d_{eq}\times w$) with $d_{eq} = \Sigma_j d_{Ag,j} = 68$ nm, and length $l$. The higher value of the measured equivalent resistance is due to the fact that in practice the electrical conductivity of the first Ag layer having thickness of 10 nm is lower than the value measured for a 17-nm-thick film. Moreover, the effect of the contact resistance in the measurement test set up is included. The experimental results suggest that the four Ag films are in parallel with respect to the current flow along the y–direction. The resistance measurements are in fact supported by scanning electron microscopy (SEM) images which demonstrate that the Ag layers touch each other along the edges of the transparent coating.

The resulting d.c. equivalent circuit of the transparent metal of Fig.1(a) is sketched in Fig.1(b). The injected current I distributes among the Ag films according to the value of the resistances $R_{Ag,j}$ ($j$=1..4).

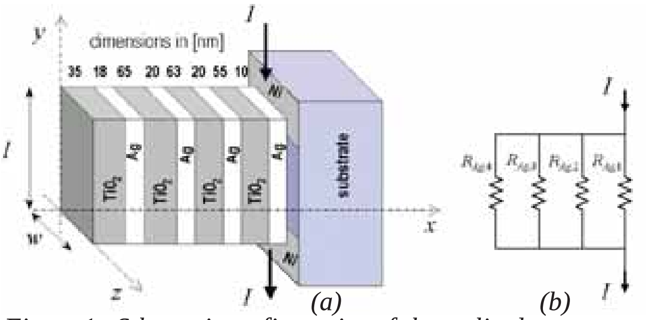


*Figure 1. Schematic configuration of the realized transparent metal specimen (a) and its equivalent d.c. circuit (b).*

### C. Optical Transparency

The optical transmittance of the transparent metal sample of Fig.1(a) is computed by using the commercial software TfCalc, and is measured for normal incidence [12]. Fig.2 shows that the maximum optical transmittance reaches the 70%.

However, it should be observed that the installation of the transparent metal of Fig.1(a) on a plain transparent substrate to realize the current path of the active shield as sketched for instance in Fig.3 would modify the chromatic resolution and luminosity of the transparent window. In the example the active shield currents are $I_1$, $I_2$, $I_3$.

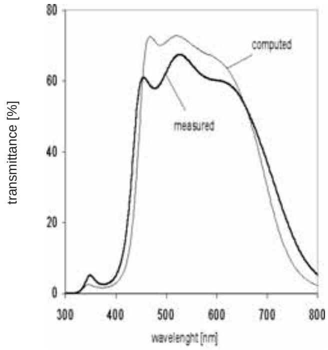


*Figure 2. Optical transmittance of the realized transparent metal sample as a function of the wavelength in free space.*

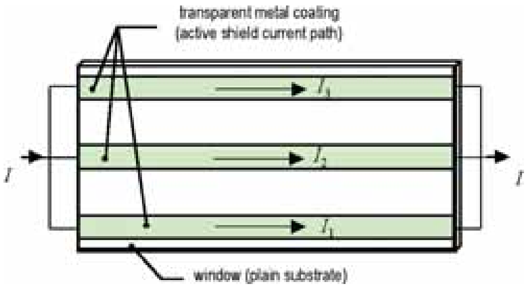


*Figure 3. Sketch of the current path of the transparent active shield coated on a plain substrate.*

In order to overcome such a problem, a suitable dielectric optical filter, having the same transmission curve of the transparent metal in the visible range, is designed by using TfCalc. The optical filter is applied on the plain transparent substrate of the screened window in order to produce the same chromatic resolution and luminosity of the transparent metal. An example of dielectric optical filter is reported in Table I. The corresponding transmittance curve is shown in Fig.4.

### D. Current Carrying Capability

The ampacity of the transparent metal sample, i.e. the maximum allowed current, depends on the thermal limit of the material. In fact, the current flow produces the increase of the temperature of both the film and the substrate. The thermal limit is the maximum working temperature below which the film integrity is not compromised. The material degradation due to overheating can be originated by three main concurring factors:

a) The film detachment from the substrate; this occurs in general at lower temperature in the case of plastic or polymeric substrates characterized by relatively low melting point (from about 120°C of polyethylene to higher values).
b) The formation of islands in the Ag film; this phenomenon, which occurs at lower temperature as the film thickness decreases towards the limit of 10 nm, produces the dramatic reduction of the electrical conductivity of the Ag film. Experimental studies have demonstrated that in thin films, with thickness up to a few tens of nanometers, the Ag aggregation in islands is always observed for temperature higher than 200°C, whereas it never takes places below 50°C.
c) The complete fusion of the Ag layers: this occurs at temperature close to the melting point of silver.

*TABLE I. LAYER COMPOSITION AND THICKNESS OF THE DIELECTRIC FILTER WITH TRANSMISSION SPECTRUM THAT WELL APPROXIMATES THE ONE OF THE TRANSPARENT METAL.*

| **Layer sequence** |
|---|
| Ti\|$SiO_2$\|$TiO_2$\| $SiO_2$\|$TiO_2$\| $SiO_2$\|$TiO_2$\| $SiO_2$\|$TiO_2$\| $SiO_2$\|$TiO_2$\| $SiO_2$\|Ti\| $SiO_2$\|$TiO_2$\| Ti\| $SiO_2$\|$TiO_2$\| $SiO_2$ |
| **Thickness [nm]** |
| 1 \| 152 \| 93 \| 150 \| 76 \| 147 \| 69 \| 169 \| 131 \| 44 \| 45 \| 16 \| 1 \| 14 \| 51 \| 1 \| 47 \| 27 \| 126 |

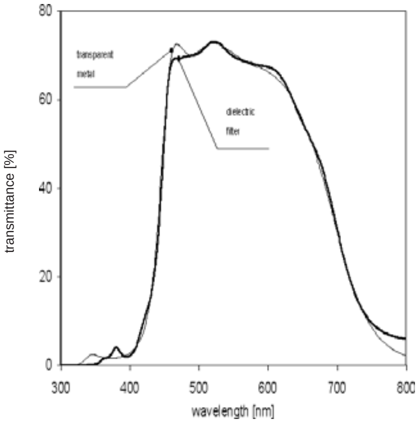


*Figure 4. Computed optical transmittances of the transparent metal and of the dielectric filter as a function of the wavelength in free space.*

In order to avoid the transparent metal degradation due to the thermal stresses, the numerical prediction of the temperature distribution along the nanolayered coating is performed as function of the injected current. A rigorous simulation model based on the solution of the one-dimensional heat diffusion equation for a multilayered planar structure is developed. However preliminary numerical calculations have demonstrated that for a very thin film the temperature variation along the different layers is not significant. Therefore, the thermal balance of a single Ag layer with equivalent thickness $d_{eq}$ of 68 nm produces a good approximation of the ampacity of the transparent metal, as function of the maximum working temperature. The error due to the approximation is limited to 2%. At steady state conditions, the internally generated heat caused by the Joule losses must equal the total output heat due to convection and radiation. The heat balance equation to calculate the film's current-carrying limit $I_L$ is:

$$R_{eq,M} I_L^2 = hS(T_{Ag} - T_e) \tag{2}$$

where $R_{eq,M}$ is the Ag layer equivalent resistance at the maximum working temperature $T_{Ag}$ of the Ag film, $h$ is the effective heat transfer coefficient, $S$ is the area of the convection and radiating surface of the film, $T_e$ is the temperature of the fluid (air) surrounding the conductor. In the case of a conductor with rectangular cross-section having thickness $d_{eq}$ and width $w$, with $d_{eq} << w$, it results:

$$I_L = \sqrt{\frac{2h(w + d_{eq}) w d_{eq} \sigma_{Ag}(T_{Ag} - T_e)}{1 + \alpha_{Ag}(T_{Ag} - T_e)}} \tag{3}$$

where $\alpha_{Ag}$ is the temperature coefficient of the Ag film, and $\sigma_{Ag}$ the electrical conductivity at temperature $T_e$.

The coefficient $h$ depends on many factors like the thermal and dynamical properties of the fluid, the geometrical configuration and the heat absorption coefficient of the material sample. In case of natural convection, typical values of $h$ range from 5 to 25 W/m$^2$K. The coefficient $\alpha_{Ag}$ can be assumed equal to 3.8·10$^{-3}$ K$^{-1}$.

Fig.5 shows the current $I_L$ of the transparent metal sketched in Fig.1 (a), having the total Ag thickness of 68 nm, as function of the sample width $w$. The obtained curves are computed assuming the environment temperature of 25°C and $h$=5 W/m$^2$K or $h$=10 W/m$^2$K and considering three different values of maximum working temperature $T_{Ag}$, namely 100°C, 125°C and 150°C. The lowest value of temperature applies in the case of plastic substrate with low melting point; the highest one in the case of glass substrate.

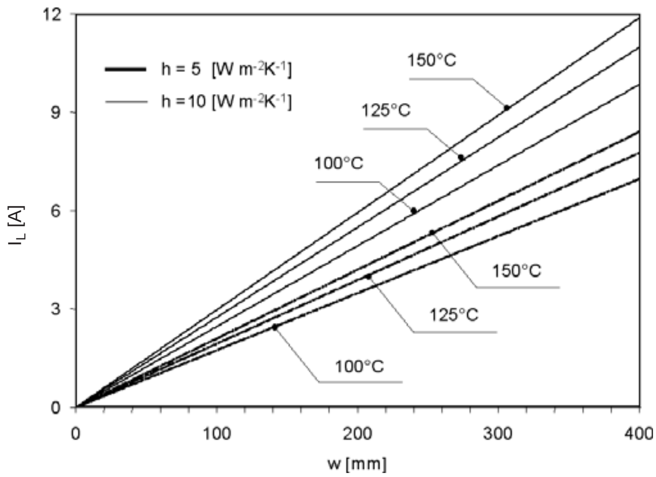


*Figure 5. Current at thermal limit as function of the sample width.*

## III. ANALYSIS OF THE SHIELDING PERFORMANCES OF TRANSPARENT METAL ACTIVE SCREENS

Numerical calculations are carried out with the aim of assessing the performances of the innovative active shield described above.

### A. Test Configuration

The test configuration sketched in Fig.6 is considered: the wire carrying the a.c. current at 50 Hz with rms value $I_s$=25 A, is centered in the rectangular 2D-enclosure of dimensions ($a$=50 cm)×($b$=30 cm), having an aperture of width $c$=40 cm centered along the wall located at $x$=0. The enclosure is assumed to be made of perfect-electric-conducting (PEC) material. Therefore, the low-frequency magnetic field couples from the inside to the outside only through the unscreened aperture. The magnetic field induction B is monitored along the $z$-axis, at the distance $p$= 5 cm from the aperture.

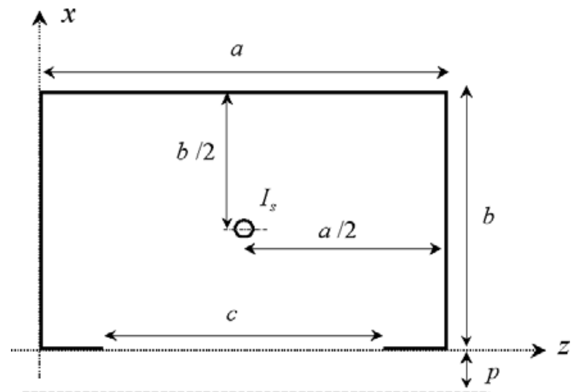


*Figure 6. 2D-test enclosure with aperture of width c.*

Different active shield configurations, using the transparent metal coating sketched in Fig.1(a) as current path, are simulated. The sensitivity analysis of the shielding performances of the proposed screening solutions is performed as function of the active shield configuration and enclosure dimensions.

It should be observed that the considered configuration represents a critical test case due to the following reasons. First, the unipolar current source produces along the aperture a magnetic field distribution that is characterized by high non-uniformity. Second, the aperture to be screened is located at only 15 cm from the source. Third, the aperture is relatively wide compared with the enclosure dimension $a$.

### B. Active shield design

One of the main mechanisms at the basis of the low-frequency magnetic field shielding is the eddy-current phenomenon. Perfect passive shielding is achieved in theory when the installed screen, in a close configuration, allows the circulation of the eddy-current amount that produces the complete cancellation of the magnetic field originated by the source.

In the case of low-frequency magnetic field shielding by using non-magnetic materials, the eddy currents are limited mainly by the screen thickness and electrical conductivity. Then, transparent metals are not suitable for low frequency passive shielding because of the very small overall thickness of the Ag layers (only 68 nm in total), even if the electrical conductivity of the Ag film, $\sigma_{Ag}$, is relatively high. The transparent metal is used for active shielding by the injection of the necessary amount of current that produces the required attenuation of the source magnetic field, taking into account the thermal limit of the material.

The first step of the active shield design consists in determining the amplitude and phase distributions of the induced current density $J_p$ in a passive shield, which produces the required attenuation of magnetic field. The second step consists in the sizing of the transparent metal coating to be deposited on the plain substrate to be shielded in order to reproduce the effect of the simulated passive shielding by enforcing the computed eddy current, and taking into account the thermal constraint.

## C. Numerical results

Numerical simulations are performed using the commercial code Ansoft Maxwell 2D [13] by assuming that the aperture in the test configuration of Fig.6 is shielded with a conducting panel of thickness $d_p$=1 mm and electrical conductivity ranging from $\sigma_{Ag}$ to 50 $\sigma_{Ag}$. The inner current source at 50 Hz has rms value of 25 A. It results that the computed current density $J_p$ induced in the thin passive shield is characterized by a uniform distribution along the $x$-axis of the screen cross-section.

Numerical experiments have demonstrated that for conductivity higher than 50 $\sigma_{Ag}$ the amplitude of the eddy current density induced in the screen saturates, whereas the corresponding phase constant approaches 180°.

Fig.7 shows the distribution, along the $z$-axis at $x$=-$p$, of the magnetic induction amplitude without the screen and with the passive shields.

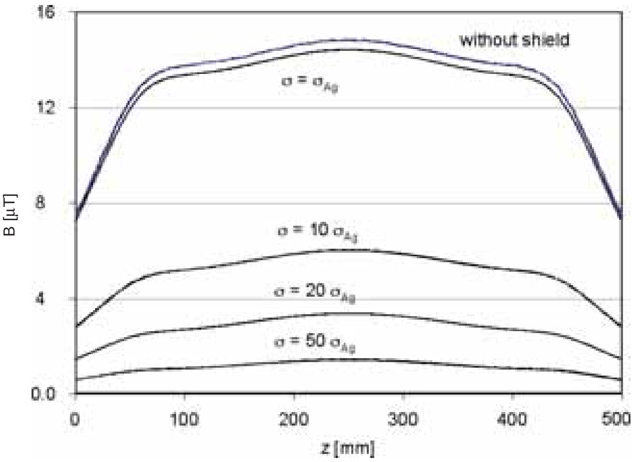


*Figure 7. Profile of the magnetic induction along the z-axis at x=-p, without shield and in presence of a passive shield having different values of electrical conductivity.*

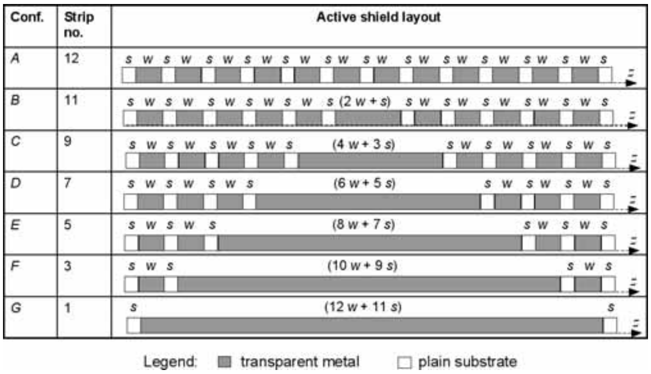


*(a)*

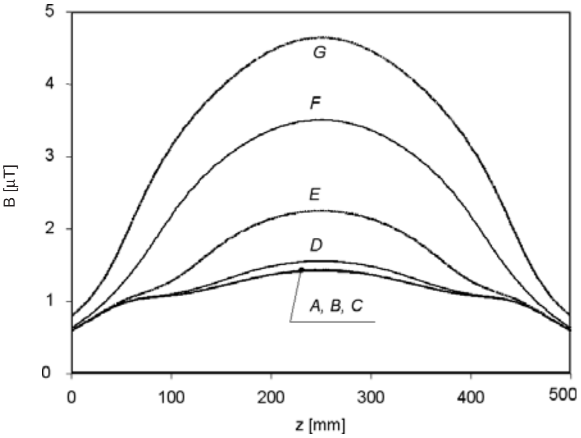


*(b)*

*Figure 8. Schematic representation of the simulated active shield configurations (a), and computed profiles of the magnetic induction along the z-axis at x=-p (b).*

Successively, the active shield that well approximates the performances of the passive screen with conductivity 50 $\sigma_{Ag}$ is modeled. Since it is unfeasible to reproduce with a single active shield the distribution of the current density calculated in the passive shield along the $z$-axis, it is necessary to divide the transparent metal in $n$ strips, located at a distant $s$ each from the other. The current $I_j$ injected in the $j$-th strip is given by

$$I_j = d_p \int_{jc/n}^{(j-1)c/n} J_p dz \qquad j = 1..n \tag{4}$$

where $c$ is the width of the enclosure aperture. It is clear that for $n \to \infty$ and $s \to 0$ the distribution of the current along the active shield approaches the passive shield one.

Good results are obtained by assuming that the unscreened window is coated by 12 strips of transparent metal having width $w$=30.3 mm and $s$=2.8 mm apart (configuration $A$ in Fig.8(a)). Due to the symmetry of the test configuration, only the first six injected currents are shown in amplitude and phase in Tab II: $I_1$ is the current in the first left-side strip, $I_6$ is the current in the central one. It should be observed that the current injected in the central strips ($I_6$) overcomes the value of 0.89 A in Fig.5, corresponding to the highest thermal limit of the material computed for $T_{Ag}$=150°C and $h$=10 W/m²K.

The resulting magnetic induction along the $z$-axis at $x$=-$p$ reported in Fig.8(b) (curve A) is nearly overlapping with the corresponding profile obtained in Fig.7 for 50 $\sigma_{Ag}$.

Successively, the active shield layouts from *B* to *G* in Fig.8(a) are considered in order to reduce the thermal solicitation on the central strips. To this end, the most solicited current paths are grouped. The resulting current to be injected is computed as sum of the current in each strip of the group.

The corresponding profiles of magnetic induction along the *z*-axis at *x*=-*p* are reported in Fig.8(b). Notice that the curves referring to configurations *A*, *B*, *C* are nearly overlapping. Moreover, only in layout *G* the enforced current is below the value of 9.7 A, corresponding to the thermal limit at 100°C and for *h*=10 W/m$^2$K.

In order to optimize the shield performance, it is assumed that the current injected in configuration *G* is opposite in phase with respect to the source current $I_s$ and has increasing rms value from 10 A to 13 A.

The results reported in Fig.9 show that a good compromise between maximum field attenuation and uniformity along *z*-axis is obtained for current ranging from 11 A to 12 A.

Finally, the geometry is modified by increasing the size of *b* up to 60 cm, so that the active screen is farther from the source. Fig.10 shows the computed magnetic field profile along the *z*-axis at *x*=-*p* in the following configurations: unscreened aperture, active shield layout *A*, and active shield layout *G* without or with optimization of screening performances. In this case the injected current in the screen is always below the thermal limit.

*TABLE II. CURRENTS INJECTED IN THE FIRST SIX STRIPS OF THE ACTIVE SHIELD HAVING THE CONFIGURATION A IN FIG.8(A).*

| | $I_1$ | $I_2$ | $I_3$ | $I_4$ | $I_5$ | $I_6$ |
|---|---|---|---|---|---|---|
| rms [A] | **0.27** | 0.49 | **0.71** | **0.95** | **1.17** | 1.31 |
| phase | 172.7° | 178.3° | 177.5° | **176.1°** | **174.7°** | 173.9° |

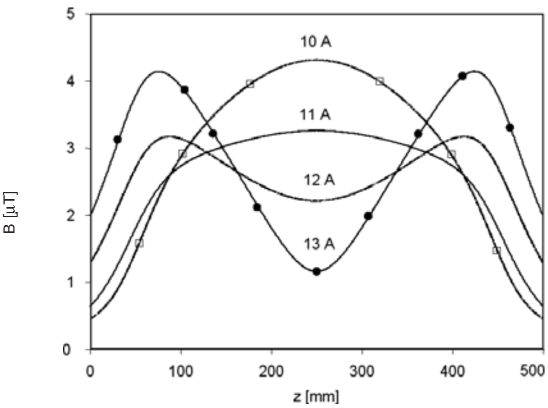


*Figure 9. Profiles of the magnetic induction computed along the z-axis at x=-p in the active shield configuration G of Fig.8 (a), for different values of the injected current.*

## IV. CONCLUSIONS

An innovative active shielding technique against low-frequency magnetic field is proposed. Transparent nanostructured thin films, constituted by alternating layers of silver and titanium oxide, are used to realize the active shield current paths instead of bulk conductors, which constitute an optical barrier. A sample of transparent metal deposited on glass substrate is realized at the Thin Film Laboratory of ENEA Casaccia. The electrical and optical properties of the specimen are assessed by experimental tests. It results that the maximum optical transmittance

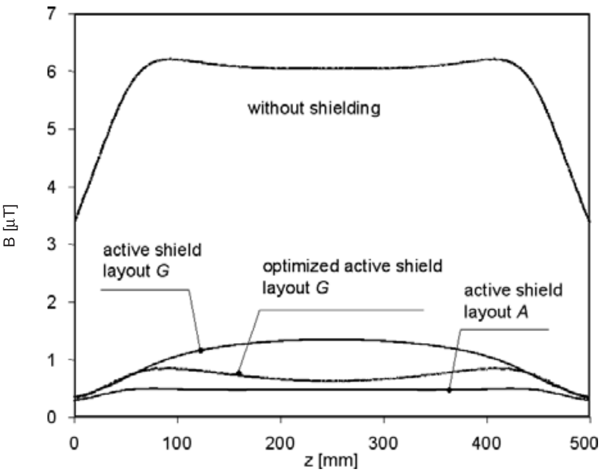


*Figure 10. Profile of the magnetic induction along the z-axis at x=-p for the 2D-enclosure with b=60 cm, without shield and in presence of different active shield configurations.*

of the transparent metal reaches 70% for normal incidence. Moreover, all silver films in the coating are in parallel with respect to the current flow in d.c. condition.

The most critical aspect in the active shield design is related to the definition of the maximum current at thermal limit, which depends on the maximum working temperature, active shield configuration, environmental conditions.

Numerical applications demonstrate the feasibility of the proposed shield solution with reference to a 2D-test enclosure with an optical aperture, excited by an inner a.c. current source at 50 Hz. The performance of the proposed active shield improves as the distance from the source and the surface of the current path increase.

## REFERENCES


[1] S. Celozzi, M. D'Amore, "Magnetic field attenuation of nonlinear shields", IEEE Trans. on EMC, Vol.33, No.3, Aug. 1996, pp.318-326.

[2] B.A. Clairmon, R.J. Lordan, "3-D modeling of thin conductive sheets for magnetic field shielding: calculation and measurements", IEEE Trans. on Power Delivery, Vol.14, Oct. 1999, pp.1382-1391.

[3] M. Istenic, R.G. Olsen, "A simple hybrid method for ELF shielding by imperfect finite planar shields", IEEE Trans. on EMC,Vol. 46, No.2, May 2004, pp. 199 – 207.

[4] M. L. Hiles, R.G. Olsen, K.C. Holte, D. R. Jensen, K.L. Griffing, "Power frequency magnetic field management using a combination of active and passive shielding technology", IEEE Trans. on Power Delivery, Vol. 13, No. 1, Jan. 1998, pp.171-179.

[5] M.D'Amore, S. Grifa, F. Maradei, "Shielding techniques of power frequency magnetic field aboard high speed train", Int. Symp. EMC Europe 2004, Eindhoven, The Netherlands, Sept. 6-10, 2004, pp. 524-529.

[6] M.D'Amore, M.S. Sarto, F. Sarto, M. Bertolotti, M.C. Larciprete, M. Scalora, C. Sibilia, "Nanotechnology of transparent electromagnetic shields", 15th Int. Zurich Symp. & Techn. Exhibition on EMC, Zurich, Switzerland, Febr. 18-20, 2003.

[7] M.S. Sarto, F. Sarto, M.C. Larciprete, M. Scalora, M. D'Amore, C. Sibilia, M. Bertolotti, "Nanotechnology of transparent metals for radio frequency electromagnetic shielding", IEEE Trans. on EMC, November 2003.
[8] M. Bloemer, M. Scalora, "Transmissive properties of Ag/Mgf2 photonic band gaps", Appl. Phys. Lett., Vol. 72, No. 14, 1998, pp. 1676-1678.
[9] Silver in Handbook of optical constants of solids II, E.D.Palik ed., Academic Press Inc., New York, 1991, pp. 350-357.
[10]Zinc oxide (ZnO) in Semiconductors II-VI and I-VII Compounds; Semi-magnetic Compounds, Numerical data and functional relationships in science and technology, Landolt-Börnstein-Condensed Matter III/41B, 1999.
[11]M.S. Sarto, R. Li Voti, F. Sarto, M.C. Larciprete, "Nanolayered lightweight flexible shields with multidirectional optical transparency", Vol. 47, No. 3, Aug. 2005, pp. 602-611 IEEE Trans. on EMC.
[12]M.S. Sarto, F. Sarto, A. Tamburrano, "Shielding performances of innovative transparent metals against radio frequency EM fields", 2004 IEEE Int. Symp. on EMC, S. Clara, CA, Aug. 2004.
[13] Maxwell 2D, Ansoft Corporation, User Manual.

## Author Biographies

*Marcello D'Amore is full professor of Electrotechnics and Electromagnetic Compatibility at the Faculty of Engineering of the University of Rome "La Sapienza" where he was head of the Electrical Engineering Department from 1983 to 1985 and from 1989 to 1995. He has published more than 150 papers in the field of electromagnetic compatibility (EMC) and power line communication (PLC). Current research interests include electromagnetic modeling of carbon nanotubes, electromagnetic hazards aboard aircraft, and EMC of broadband PLC. He was chairman of the International Symposia EMC ROMA '94, '96, '98, and of the International Steering Committee of the EMC EUROPE 2000, 2002, and 2004. He was guest editor of the 1996 Special Issue "EMC Research in Italy", guest co-editor of the 1998 Special Issue "Lightning", and Editor-in-Chief from 2000 to 2003 of IEEE Transactions on EMC. He received the Best Paper Award of the IEEE International Symposium on EMC, Dallas 1993 and Chicago 2005, and of the ISH'97, Montreal, the IEEE EMC Society 1997 and 2001 Transactions Prize Paper Awards, and the 2003 Richard R. Stoddart Award, and the SAE 2001 Wright Brothers Medal. He is Fellow of the IEEE since 1990.*

*Maria Sabrina Sarto (Ph.D. in Electrical Engineering in 1997) is Full Professor in Electrotechnics and EMC since 2004 at the University of Rome "La Sapienza." She has been Director of the EMC Laboratory of the Department of Electrical Engineering since 1999, Director of the Research Centre on Nanotechnology Applied to Engineering of the University of Rome "La Sapienza" (CNIS) since 2006, and Director of the Joint Lab on Micro & Nanotechnology for Industrial Engineering of La Sapienza University since 2007. She is author of more than a hundred scientific papers, covering several EMC topics and she is author of over a hundred technical and scientific papers, covering several EMC topics and nanotechnology. Her recent research interests include carbon nanotube EM modeling, nanostructured material for EMI shielding, nano-transmission lines, absorbing materials and thin films, EMC on aircraft, numerical modeling, and EM characterization of materials. She received from the IEEE EMC Society the President's Memorial Awards in 1996 and 1997, the 1997 and the 2000 Prize Paper Award of IEEE Transactions on Electromagnetic Compatibility, as well as the 1993 and 2004 IEEE EMC Symposium Best Paper Awards. In 2001, she received from the SAE the Wright Brothers Medal Award. She has been Associate Editor of the IEEE Transactions on Electromagnetic Compatibility since 1999 and a Senior Member of IEEE since 2001. She was a Distinguished Lecturer of the IEEE EMC Society in 2001-2002. She is Chairman of the Working Group IEEE Std. 299.1, Representative of the IEEE EMC Society in the Nanotechnology Council for the years 2005-2006, and Chairman of the Nanotechnology Working Group of AEIT-ASTRI.*

*Alessio Tamburrano received the laurea, summa cum laude, and the Ph.D. degrees in electrical engineering from the University of Rome "La Sapienza" in 2003 and 2007, respectively. Since 2006, he has been Assistant Professor at the Department of Electrical Engineering, University of Rome "La Sapienza" in Italy. His research activity is focused on electromagnetic compatibility and nanotechnology, and current interests include electromagnetic characterization of transparent thin films, nanostructured and composite shields, nano-transmission lines and diagnostics of the wiring system aboard aircraft. He received the IEEE EMC Society Best Paper Award at the 2005 IEEE International Symposium on EMC in Chicago, Illinois. He is a Registered Professional Engineer in Italy, and is a member of the IEEE EMC Society.*

*Francesca Sarto has the degree in Physics, and has been working in ENEA since 1993, as researcher. She has been dealing with PVD techniques, in particular with sputtering and ion assisted techniques. Her main interest is the study of the physical mechanisms occurring during the film growth, in order to correlate the film properties to the deposition parameters. In particular, her research activity has been focused on the study and the improvement of the adhesion properties of single layer and multi-layer coatings deposited on plastic substrates. She has carried out her research activity in the framework of national and European projects, in collaboration with academic and industrial partners, and published over fifty technical and scientific papers on this topics on international journals or in the proceedings of international symposia.* EMC